Hindawi Publishing Corporation
Journal of Structures
Volume 2013, Article ID 176739, 12 pages
http://dx.doi.org/10.1155/2013/176739

Research Article

Effects of Side Ratio on Wind-Induced Pressure Distribution on Rectangular Buildings

J. A. Amin[1] and A. K. Ahuja[2]

[1] *Department of Civil Engineering, Sardar Vallabhbhai Patel Institute of Technology, Vasad 388 306, India*
[2] *Department of Civil Engineering, Indian Institute of Technology Roorkee, Roorkee 247 667, India*

Correspondence should be addressed to J. A. Amin; jamin_svit@yahoo.com

Received 25 February 2013; Revised 27 June 2013; Accepted 11 July 2013

Academic Editor: Vincenzo Gattulli

This paper presents the results of wind tunnel studies on 1 : 300 scaled-down models of rectangular buildings having the same plan area and height but different side ratios ranging from 0.25 to 4. Fluctuating values of wind pressures are measured at pressure points on all surfaces of models and mean, maximum, minimum, and r.m.s. values of pressure coefficients are evaluated. Effectiveness of the side ratios of models in changing the surface pressure distribution is assessed at wind incidence angle of 0° to 90° at an interval of 15°. Side ratio of models has considerable effects on the magnitude and distribution of wind pressure on leeward and sidewalls but it has very limited effect on windward walls at wind incidence angle of 0°. For building models with constant cross section, change in side ratio does not significantly affect the general magnitude of peak pressures and peak suctions, but rather the wind angle at which they occur. The regression equation is also proposed to predict the mean pressure coefficient on leeward wall and side wall of rectangular models having different side ratios at 0° wind incidence angle.

1. Introduction

Generally, flexible high rise structures are susceptible to excessive levels of vibration under the action of wind, causing discomfort to building occupants and posing serious serviceability issue, which govern the design of lateral system and claddings. While designing high rise buildings and their cladding for wind load, the designers refer to the relevant standard IS: 875 part 3 [1], AS/NZS: 1170.2 [2], and ASCE: 7-02 [3] to pick the wind pressure coefficients and wind force coefficients. Most of the Standards/Codes of Practice for Design Loads (Wind Loads) for Building and Structures suggest the design pressure coefficients and force coefficients for square and rectangular buildings having different side ratios and height at specific wind incidence angle, but they do not suggest the pressure coefficients on too elongated rectangular plan shape buildings and pressure coefficient at skew wind incidence angles.

Furthermore, the loads from codes are meant to be upper bound scenario covering almost all cases. However, note the following limitations of the building codes/standards. Wind load/pressure information (i) does not consider the aerodynamic effect of the actual shape of the structure since it is based on box-like buildings and (ii) does not allow for any detailed directional effects and assumes that the design wind speed will always occur from the aerodynamically severe wind direction. On the other hand, wind tunnel model studies, which are often used to assist in the prediction of the design wind loads for the cladding and structural frame specifically on tall buildings, (i) do physically simulate and predict the aerodynamics effect of the actual shape of the structure by modeling building in detail and (ii) overall provide indispensable wind-effect data for the design of the cladding and structural frame work.

During the past decades, investigators attempted to determine the overall mean and fluctuating drag and lift forces as well as fluctuating pressures at various locations on prismatic bluff bodies. However, few studies have been reported involving investigating the effects of side ratio and wind orientations on the wind pressure distributions of rectangular model through wind tunnel test. Vickery [4], Lee [5], and Miyata and Miyazaki [6] measured steady and

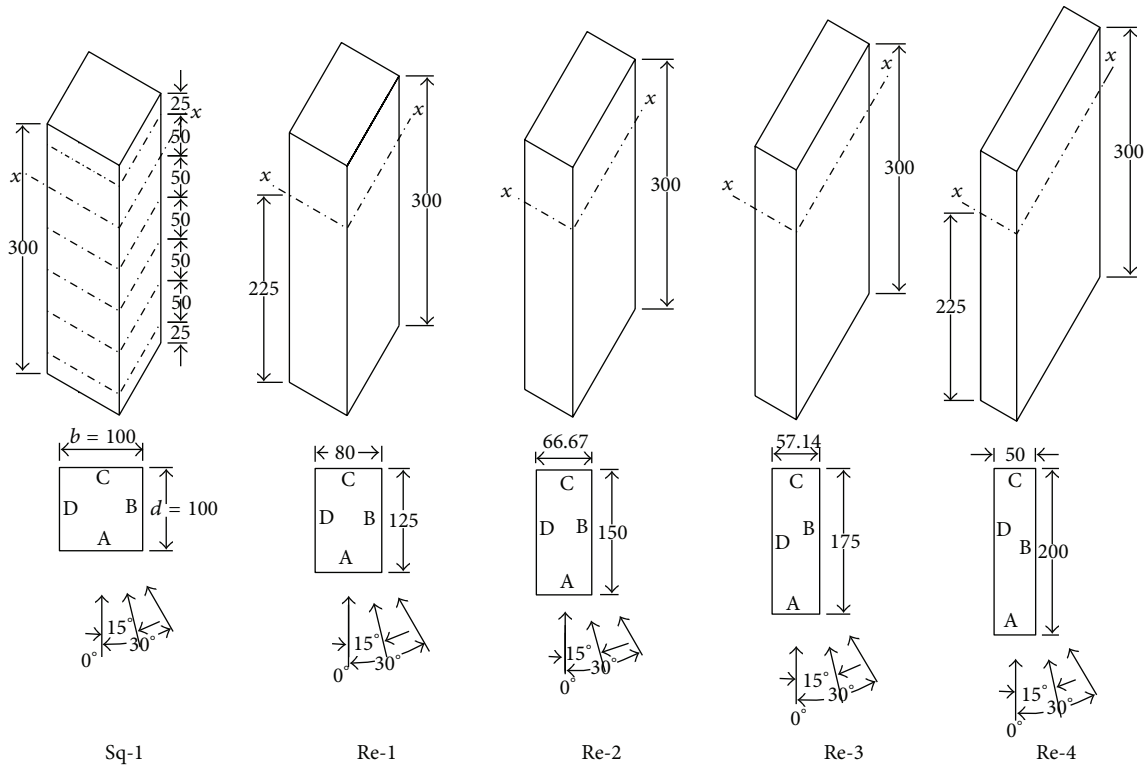

(a)

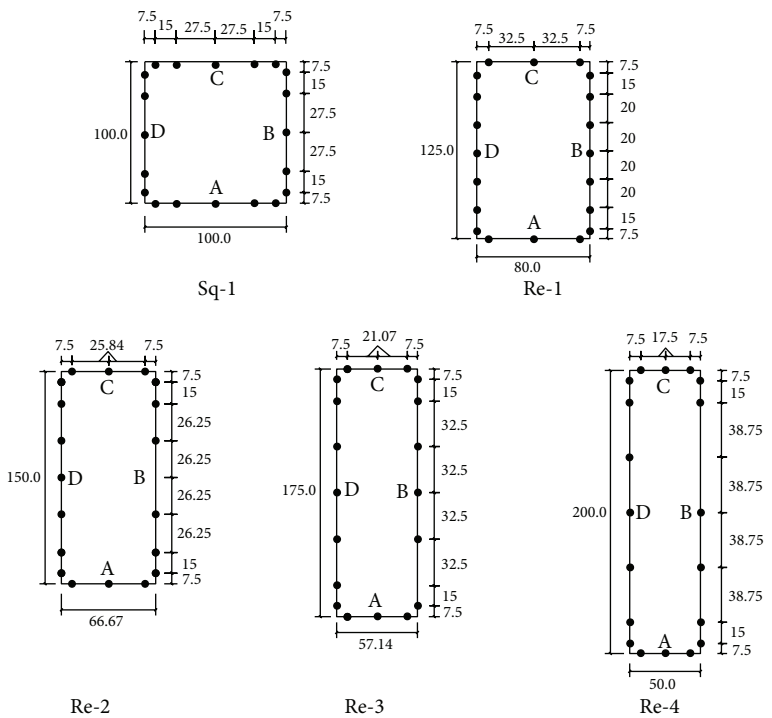

(b)

Figure 1: (a) Plan and isometric view of building models. (b) Pressure tapping locations along the perimeter of building models.

Table 1: Dimensions and designation of building models.

Model shape and designation	Wind angle	Width (mm)	Depth (mm)	Height H (mm)	Side ratio	Aspect ratio
Square (Sq-1)	0°	100	100	300	1	3
Rectangular-1 (Re-1)	0°	80	125	300	1.56	3
Rectangular-2 (Re-2)	0°	66.67	150	300	2.25	3
Rectangular-3 (Re-3)	0°	57.14	175	300	3.06	3
Rectangular-4 (Re-4)	0°	50	200	300	4	3
Rectangular-1 (Re-1)	90°	125	80	300	0.64	3
Rectangular-2 (Re-2)	90°	150	66.67	300	0.44	3
Rectangular-3 (Re-3)	90°	175	57.14	300	0.33	3
Rectangular-4 (Re-4)	90°	200	50	300	0.25	3

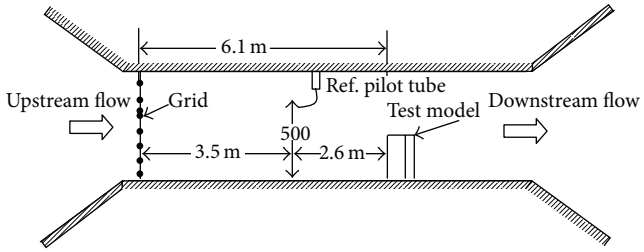

Figure 2: Schematic line diagram of wind tunnel.

unsteady surface pressures and spatial correlations in two-dimensional flows. Lee concluded that an increase on the turbulence intensity in the flow normal to the prism produces complete pressure recovery on the side faces and a reduction in the base pressure. Kareem and Cermak [7] investigated the pressure distribution on sidewalls of a square model in the different boundary layer flow conditions of suburban and urban terrain. The general characteristics of the 2D separation/reattachment process and the generation of peak suctions have also been observed in the work of Saathoff and Melbourne [8] using similar models of square prisms and of long flat plates with rectangular leading edges. Kareem [9] investigated the influence of turbulence on the space-time structure of random pressure field on the surface of prismatic bluff bodies exposed to turbulent boundary layer flows. Surry and Djakovich [10] explore the high peak suctions developed on the building models and their relationship with building shape and characteristics of the oncoming simulated atmospheric flow. Li and Melbourne [11, 12] investigated the effects of turbulence length scale on the maximum and minimum pressure acting on the side surfaces of rectangular models. Kim et al. [13] investigated the effects of side ratios on across-wind pressure distribution on rectangular tall buildings. Lin et al. [14] tested nine models of different rectangular cross sections in a wind tunnel to investigate the effects of three parameters, namely, elevation, aspect ratio, and side ratio, on bluff-body flow and thereby on the local wind forces. Amin [15] investigated the wind pressure distribution on rectangular tall buildings of different side ratios but having the same plan area and height.

The pressure fluctuations on the walls of a building exposed to a boundary layer results from the turbulence present in the approach flow from flow separation and reattachment, from vortex shedding in the wake and building shape, and so forth. Successful analytical prediction of wind loads has been impaired by the complex nature of wind-structure interactions. Therefore, scaled model tests of buildings in simulated boundary layer flows continue to serve as the most practical and promising means of predicting loads on structures. In the present study, the effects of side ratios and wind directions on wind pressure distribution on rectangular building models of similar plan area and height are investigated experimentally. The regression equation is also proposed to predict the mean wind pressure coefficients on leeward and side face of building models having different side ratio for open country terrain at 0° wind incidence angle.

2. Experimental Programme

2.1. Details of Models. The models used for the experiments are made of 6 mm thick transparent Perspex sheet at a same geometrical model scale with that of wind simulation that is 1 : 300. Dimensions and designation of building models are shown in Table 1. Plan area and height of all the models are kept the same at 10,000 mm^2 and 300 mm, respectively, for comparison purpose. The plan and isometric views of building models are shown in Figure 1(a). All the models are instrumented with around 150 numbers of pressure taps at seven different height levels 25, 75, 125, 175, 225, 250, and 275 mm from bottom to obtain a good distribution of pressures on all the walls of building models. These pressure taps are placed as near as possible to the edges of the faces to attempt to capture the high pressure variation at the edges of the faces. Figure 1(b) shows pressure tapping locations along the perimeter of building models.

For making the pressure points, the steel tap of 1.0 mm internal diameter is inserted into the hole drilled on the model surface such that its one end flushes to the outer side of the model surface. Another end of the steel tap is

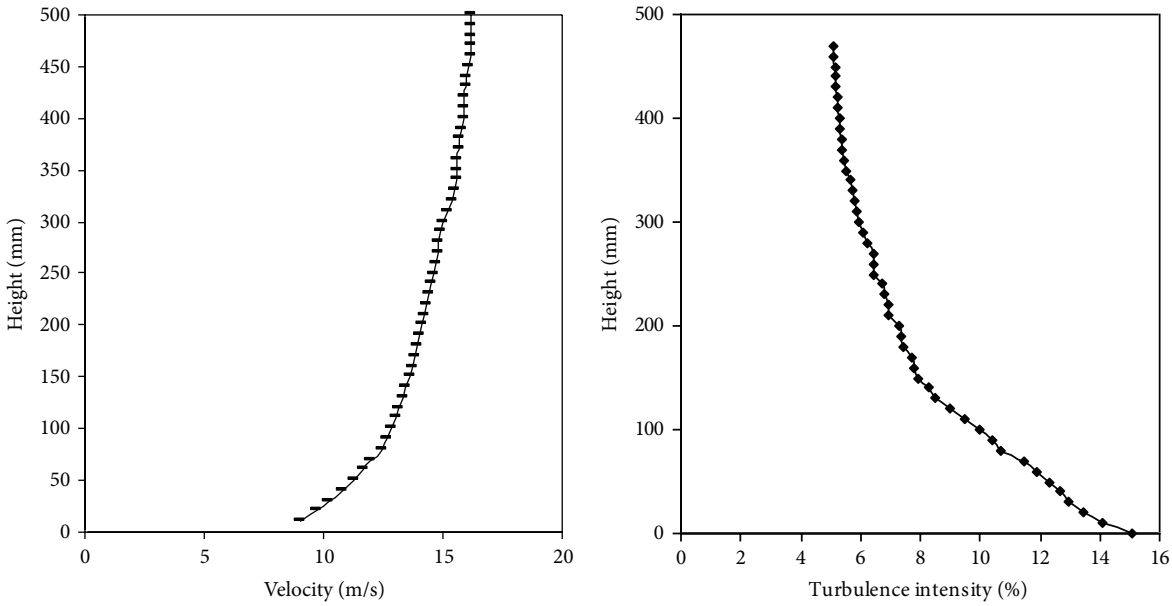

Figure 3: (a) Velocity profile at test section. (b) Turbulence intensity at test section.

connected to the vinyl tubing of 1.2 mm internal diameter. The free end of vinyl tubing is connected to Baratron pressure gauge to measure the fluctuating wind pressure at a particular point. The wind pressure on various surfaces of the building models is measured using the Baratron pressure gauge from MKS Corporation Ltd. It is a capacitance type pressure transducer capable of measuring extremely low differential pressure heads. The gauge provides the pressure reading on particular tapping on its analog scale after adjusting it to a suitable sensitivity range, which is called Baratron range. The tubing system was dynamically calibrated to determine the amplitude and phase distortion. The analog surface pressure reading from the Baratron is converted to digital reading with solid state integrator and subsequently the mean, r.m.s., maximum, and minimum pressures (N/m^2) are recorded in the computer using the data logger. Each tap is sampled for 15 seconds at 200 Hz.

2.2. Feature of Experimental Flow. The experiments are carried out in closed circuit wind tunnel under artificially generated boundary layer flow at the Indian Institute of Technology, Roorkee, India. The wind tunnel has a test section of 8.2 m length with a cross sectional dimensions of 1.2 m (width) × 0.85 m (height). The experimental flow is simulated similar to the conditions of an open country terrain with well-scattered obstructions having the height generally between 1.5 m and 10 m using a grid made of hollow aluminum tubes placed at the upstream end of the test section and natural action of the surface roughness added on the tunnel floor at a length scale of 1 : 300. The model is placed at a distance of 6.1 m from the upstream edge of the test section. A reference pitot tube is located at a distance of 3.5 m from the grid and 500 mm above the floor of wind tunnel to measure the free stream velocity during experiments. The line diagram of wind tunnel is shown in Figure 2. In the present study, the reference wind velocity has been maintained as 15 m/sec at the roof level of the model. The velocity profile inside the tunnel has a power-law index (n) of 0.143. The variation of nondimensional mean velocity and turbulence intensity is plotted in Figures 3(a) and 3(b), respectively.

3. Experimental Results and Discussion

Mean, r.m.s., maximum, and minimum pressure coefficients on all the surfaces of building models are evaluated from the fluctuating wind pressure records at all pressure points over an extended range of wind incidence angles, namely, 0° to 90°, at an interval of 15°. The general characteristics and the effect of side ratios on observed pressure distributions on building models at different wind incidence angles are summarized as follows.

Figures 4(a) to 4(e) show the mean pressure coefficient contours of models Sq-1, Re-1, Re-2, Re-3, and Re-4 at wind incidence angle of 0°, respectively. From the pressure contours of square and rectangular models, it is observed that at 0° wind incidence angle, pressure distribution and magnitude of pressure coefficients on windward wall of the models are almost independent of model depth and side ratio. But side ratio of models significantly affects the pressure distribution and magnitude of pressure coefficients on sidewall and leeward wall of the building models. Table 2 shows the comparisons of experimentally obtained wind pressure coefficients on building models at 0° wind incidence angle with the prominent wind standards and with available technical literature. The positive wind pressure is the pressure acting towards the wall, whereas the negative pressure/suction is

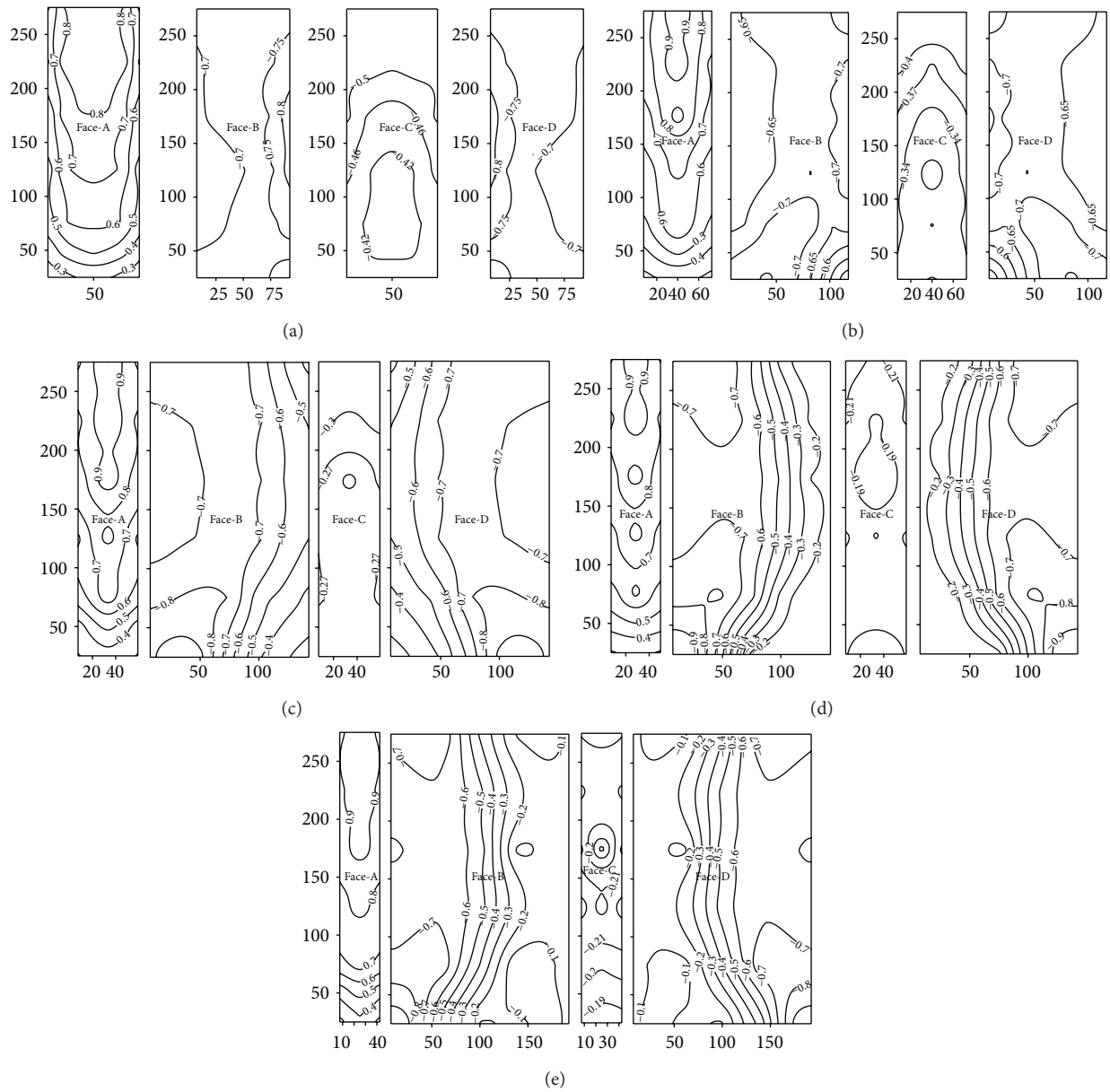

Figure 4: (a) Mean surface pressure coefficient distribution: model Sq-1 (angle 0°). (b) Mean surface pressure coefficient distribution: model Re-1 (angle 0°). (c) Mean surface pressure coefficient distribution: model Re-2 (angle 0°). (d) Mean surface pressure coefficient distribution: model Re-3 (angle 0°). (e) Mean surface pressure coefficient distribution: model Re-4 (angle 0°).

the pressure acting away from the wall of models. Indian standard IS: 875 part 3 does not suggest the mean pressure coefficients for elongated plan shape structures having side ratio of 4. From the table, it is noticed that values of negative mean wind pressure coefficients suggested by IS: 875 part 3 for building having a side ratio more than one are on lower side as compared to the experimentally observed values and values suggested by codes/standards of other countries. Table 3 shows the comparisons of pressure coefficients of square model with the results of Surry and Djakovich [10].

Figure 5 shows variation of across wind pressure coefficients on sidewalls of model at section x-x at a height of 225 mm from bottom at 0° wind incidence angle. In case of square model Sq-1 (side ratio = 1), suction on side faces increases from windward to leeward edges. In case of rectangular model Re-1 (side ratio = 1.56), suction increases almost up to 70% depth, after which it decreases slightly. In case of rectangular model Re-2 (side ratio = 2.25), suction increases almost up to 50% depth, after which it decreases. In case of rectangular model Re-3 (side ratio = 3.06), suction increases almost up to 35% depth, after which it decreases up to 90% depth and further increases slightly afterwards. In case of rectangular model Re-4 (side ratio = 4), it increases up to 30% depth, after which it decreases up to 70% depth and further increases slightly afterwards. According to the distribution of mean and r.m.s. pressure coefficients on building models, it

Table 2: Wind pressure coefficients on building models at 0° wind incidence angle.

Building model	C_p (wind pressure coefficient)	Face-A	Face-B	Face-C	Face-D
Sq-1 (side ratio = 1)	Mean	0.74	−0.69	−0.5	−0.69
	Max.	1.11	−0.6	−0.59	−0.6
	Min.	0.25	−1.1	−0.9	−1.05
	IS-875	0.8	−0.8	−0.25	−0.8
	ASCE 7-02	0.8	−0.7	−0.5	−0.7
	AS/NZS 1170.2	0.8	−0.65	−0.5	−0.65
	Macdonald (mean/max) [16]	0.8	−0.8/−1.2	−0.25	−0.8/−1.2
	Surry and Djakovich (mean) [10]	0.65	−0.7	—	−0.7
Re-1 (side ratio = 1.56)	Mean	0.74	−0.66	−0.41	−0.66
	Max.	1.11	−0.48	−0.55	−0.48
	Min.	0.31	−1.01	−0.60	−1.01
	IS-875	0.8	−0.5	−0.1	−0.5
	ASCE 7-02	0.8	−0.7	−0.4	−0.7
	AS/NZS 1170.2	0.8	−0.65	−0.4	−0.65
	Macdonald (mean/max) [16]	0.7	−0.7/−1.2	−0.4	−0.7/−1.2
Re-2 (side ratio = 2.25)	Mean	0.75	−0.62	−0.3	−0.62
	Max.	1.14	−0.26	−0.25	−0.26
	Min.	0.32	−1.09	−0.44	−1.09
	IS-875	0.8	−0.5	−0.1	−0.5
	ASCE 7-02	0.8	−0.7	−0.29	−0.7
	AS/NZS 1170.2	0.8	−0.65	−0.29	−0.65
	Macdonald (mean/max) [16]	0.7	−0.7/−1.2	−0.4	−0.7/−1.2
Re-3 (side ratio = 3.06)	Mean	0.75	−0.59	−0.2	−0.59
	Max.	1.1	−0.09	−0.15	−0.09
	Min.	0.38	−1.15	−0.25	−1.15
	IS-875	0.8	−0.5	−0.1	−0.5
	ASCE 7-02	0.8	−0.7	−0.25	−0.7
	AS/NZS 1170.2	0.8	−0.65	−0.25	−0.65
	Macdonald (mean/max) [16]	0.7	−0.7/−1.2	−0.4	−0.7/−1.2
Re-4 (side ratio = 4)	Mean	0.76	−0.55	−0.2	−0.55
	Max.	1.12	−0.09	−0.15	−0.09
	Min.	0.43	−1.07	−0.27	−1.07
	IS-875	—	—	—	—
	ASCE 7-02	0.8	−0.7	−0.2	−0.7
	AS/NZS 1170.2	0.8	−0.65	−0.2	−0.65
	Macdonald (mean/max) [16]	0.7	−0.7/−1.2	−0.4	−0.7/−1.2

is observed that reattachment of flow takes place in case of rectangular models Re-3 and Re-4 having a side ratio of 3.06 and 4, respectively. The effect of turbulence intensities in the approach flow, flow separation, and reattachment from vortex shedding that occurred in the leeward side influenced more the across wind pressure distribution.

Figure 6 shows the variation of mean wind pressure coefficients on leeward face of models of different side ratios at wind incidence angle of 0°. At wind incidence of 0°, the side ratio of models significantly affects the suction on leeward face-C. The absolute value of mean negative pressure coefficients on leeward face-C slightly increases or remains almost constant up to side ratio of 0.64. Beyond the side ratio of 0.64, the absolute values of negative pressure coefficient decrease with increasing side ratio. This suggests that as the side ratio increases beyond a critical limit value, the downstream corners will interfere with the separated shear layers and lead to reducing the suction on the rear wall.

Table 3: Pressure coefficients on building models on model Sq-1.

	At 0° wind incidence angle				
	Mean (front face)	Maximum (front face)	Peak negative (side face)	r.m.s. (side face)	Negative mean (side face)
Experimental	0.74	1.11	−1.1	0.18	−0.69
Surry and Djakovich (1995) [10]	0.65	1.1	−1.4	0.2	−0.7
	Worst maximum and minimum coefficients at all wind incidence angles				
	Maximum		Minimum		
Experimental	1.11		−1.45		
Surry and Djakovich (1995) [10]	1.1		−1.8		

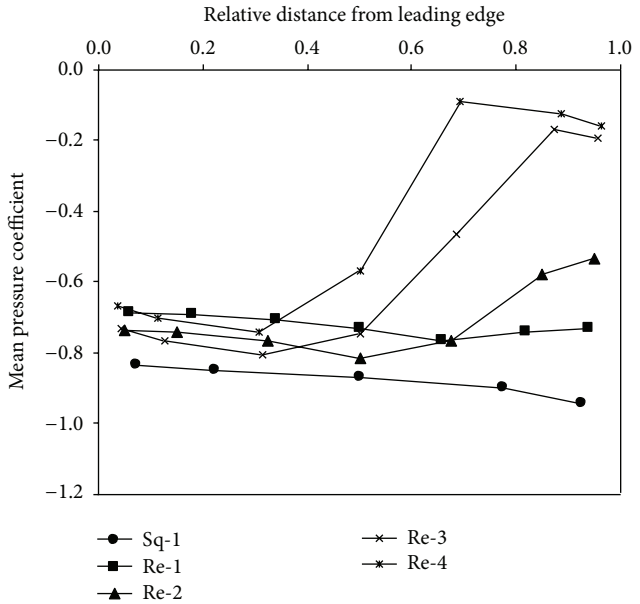

Figure 5: Mean pressure coefficients across the section x-x on side face at 0° wind incidence angle.

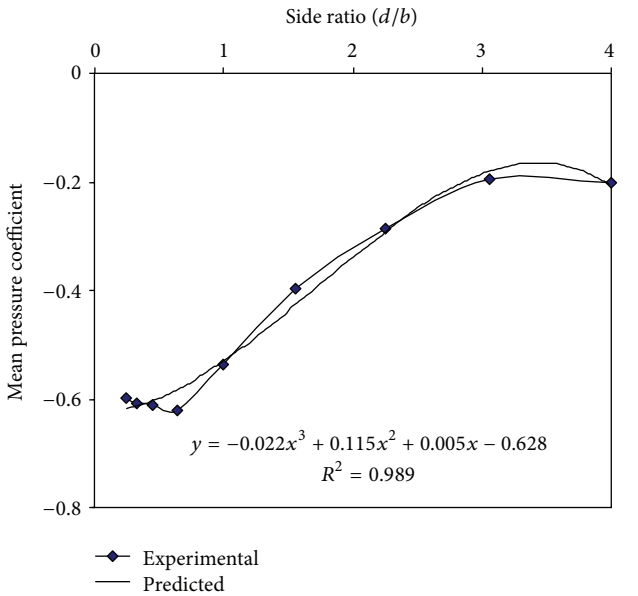

Figure 6: Variation of mean pressure coefficient on leeward face at 0° wind incidence angle.

This critical value of side ratio will change due to different free-stream turbulence intensity. Nakamura and Hirata [17] mentioned this influence of the rear corner on the shear layer and referred to it as the shear-layer-edge interaction. This interaction yields a reattachment-type pressure distribution characterized by shortened separation bubbles near the front corners followed by recovery to some higher pressure level near the rear corners. As the side ratio increases, the interaction is intensified and finally results in steady reattachment. It is observed that as the side ratio approaches to about 3.0, the final steady reattachment of the flow takes place on side faces of rectangular models at wind incidence angle of 0°. On the other hand, the negative pressure coefficient on leeward face-C becomes almost constant as the side ratio exceeds 3.0, indicating that when depth is about three times the breadth, the lower limit of the wake width, which is approximately the full width of the body, is obtained. Side ratio, however, has little influence on the variation of pressures along the vertical directions. Based on the experimental data, following regression equation is proposed to predict the mean pressure coefficient (suction) on leeward face of rectangular building models for open country terrain at 0° wind incidence angle as

$$C_p\,(\text{leeward face}) = -0.022(d/b)^3 - 0.115\left(\frac{d}{b}\right)^2 + 0.005\,(d/b) - 0.628. \quad (1)$$

Figure 7 shows the variation of weighted average mean wind pressure coefficients (suction) on side face-B and D of rectangular models having different side ratios at wind incidence angle of 0°. Based on the experimental data, following regression equation is proposed to find the average mean wind pressure coefficients on side faces of rectangular models having different side ratios for open country terrain at 0° wind incidence angle as

$$C_p\,(\text{side face}) = -0.009(d/b)^3 - 0.072\left(\frac{d}{b}\right)^2 - 0.112\,(d/b) - 0.649. \quad (2)$$

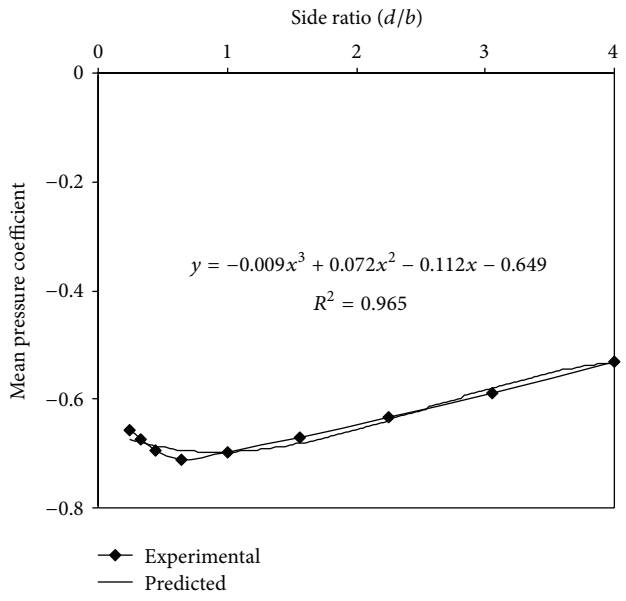

Figure 7: Variation of mean pressure coefficient on side face at 0° wind incidence angle.

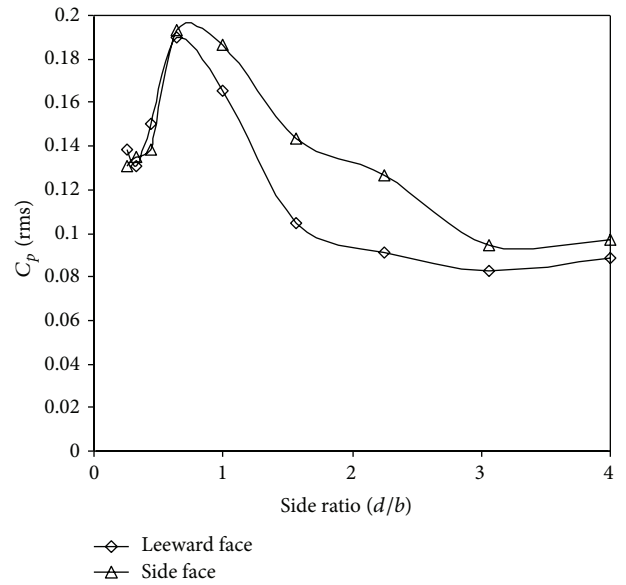

Figure 8: r.m.s. pressure coefficient on side face and leeward face at 0° wind incidence angle.

Figure 8 shows the variation of weighted average r.m.s. wind pressure coefficients on leeward and side faces of building models having different side ratios at wind incidence angle of 0°. The absolute value of r.m.s. pressure coefficients on leeward face of rectangular models increases up to side ratio of 0.64. Beyond the critical side ratio of 0.64, the absolute values of r.m.s. pressure coefficient on leeward face decreases with increases of side ratio. This suggests that as the side ratio increases beyond a critical limit value, the downstream corners will interfere with the separated shear layers and lead to reducing the fluctuation of suction on the rear wall. Beyond the side ratio of 3, r.m.s pressure coefficient on leeward face remains almost constant up to side ratio of 4. Figure 9 shows the variation of r.m.s. wind pressure coefficients at section x-x at a height of 225 mm from bottom on side faces of rectangular building models at wind incidence angle of 0°. It is noticed that the pressure fluctuations on the side faces of square and rectangular models are nonhomogenous, which implies that they are dependent on the separation distance, time, and also on the relative location of the point. As the side ratio of the models increases, the values of r.m.s. pressure coefficients on side face-B reduce at wind incidence angle of 0°.

Figure 10 shows the maximum pressure coefficient contours on face-B of models Sq-1, Re-1, Re-2, Re-3, and Re-4 at wind incidence angle of 15°. Side face-B of models Sq-1 and Re-1 is subjected to maximum negative pressure coefficient of −1.15 at wind incidence angle of 15°, without reattachment of the wind flow. At wind incidence angle of 15°, side face-B of model Re-2 is subjected maximum localized negative pressure coefficient of −1.69 near the leading edge. Indian standard for wind loads suggests the maximum localized pressure coefficient of −1.2 for similar rectangular buildings. The highest peak suctions may occur practically at any location of the model side face. However, no unusual peak values in excess of −1.69 are found. These may only be associated with more complex model geometrics with more complex surroundings. In case of rectangular models Re-2 to Re-4, the absolute values of wind pressure coefficients on side faces decrease from leading edges to the middle of the faces and then increase from middle of the faces to trailing edges at 15° wind incidence angle firstly due to the reattachment and subsequently due to separation of the flow. Figure 11 shows the r.m.s. pressure coefficient contours on face-B of models Sq-1, Re-1, Re-2, Re-3, and Re-4 at wind incidence angle of 15°.

Figure 12 shows the variation of mean wind pressure coefficients at section x-x at a height of 225 mm from bottom on side face-B of building models at wind incidence angle of 45°. It is noticed that magnitude of the mean pressure coefficient on face-B is slightly increased with increasing in side ratio of the model at wind incidence angle of 45°. The mean wind pressure coefficients on face-B of all the models are reduced from leading edge to the trailing edges and part of the wall on trailing edges is subjected to separation of the wind flow at the trailing edge. Figure 13 shows the mean pressure coefficient contours on face-C of models Sq-1, Re-1, Re-2, Re-3, and Re-4 at wind incidence angle of 45°, respectively. Suction on face-C of rectangular models Re-1 to Re-4 increases as the wind incidence angle increases from 0° to 90°. But in case of square model Sq-1, it reduces from wind incidence angle of 0° to 45° and beyond the wind incidence angle of 45°, it increases up to wind incidence angle of 90°. Higher discrepancies on the side faces may be due to the higher susceptibility of these faces to the experimental conditions like model edges, turbulence intensity, blockage effects, and so forth. As angle of wind incidence increases, the absolute value mean pressure coefficients on face-D of building models Sq-1, Re-1, Re-2, Re-3, and Re-4 are reduces up to wind incidence angle of 45°, being under the wake region influence and it is subjected to an almost uniform

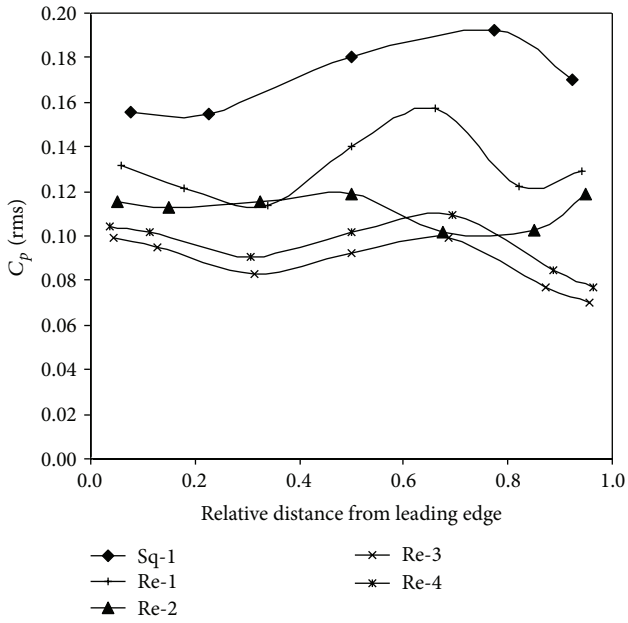

Figure 9: r.m.s. pressure coefficient on side face across section x-x at 0° wind incidence angle.

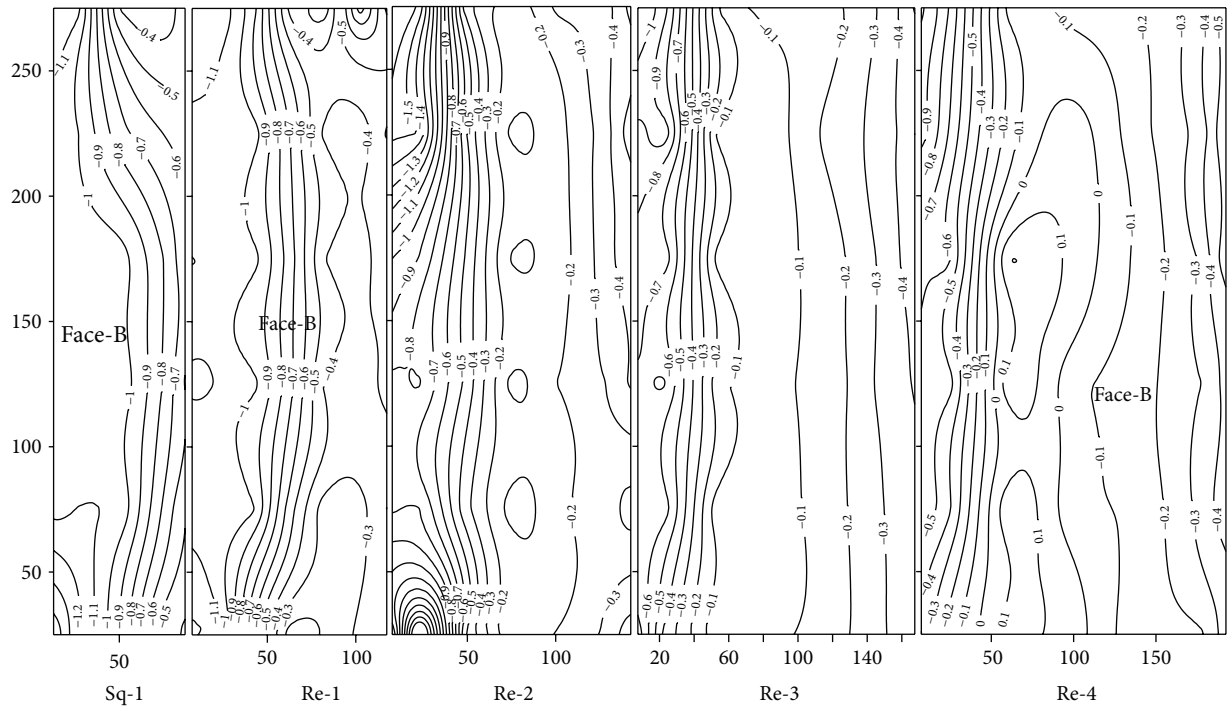

Figure 10: Minimum (peak negative) surface pressure coefficient distribution on face-B (angle 15°).

negative pressure coefficient distribution. Beyond the wind incidence angle of 45°, suction on face-D increases up to wind incidence angle of 90°.

Figure 14 shows the mean pressure coefficient contours on face-D of models Re-1, Re-2, Re-3, and Re-4 at wind incidence angle of 90°. Table 3 shows the force coefficients on building models at 0° wind incidence angle. The forces acting on the models along the wind direction are evaluated from the integration of the measured mean pressures at pressure points on all the faces of models at wind incidence angles

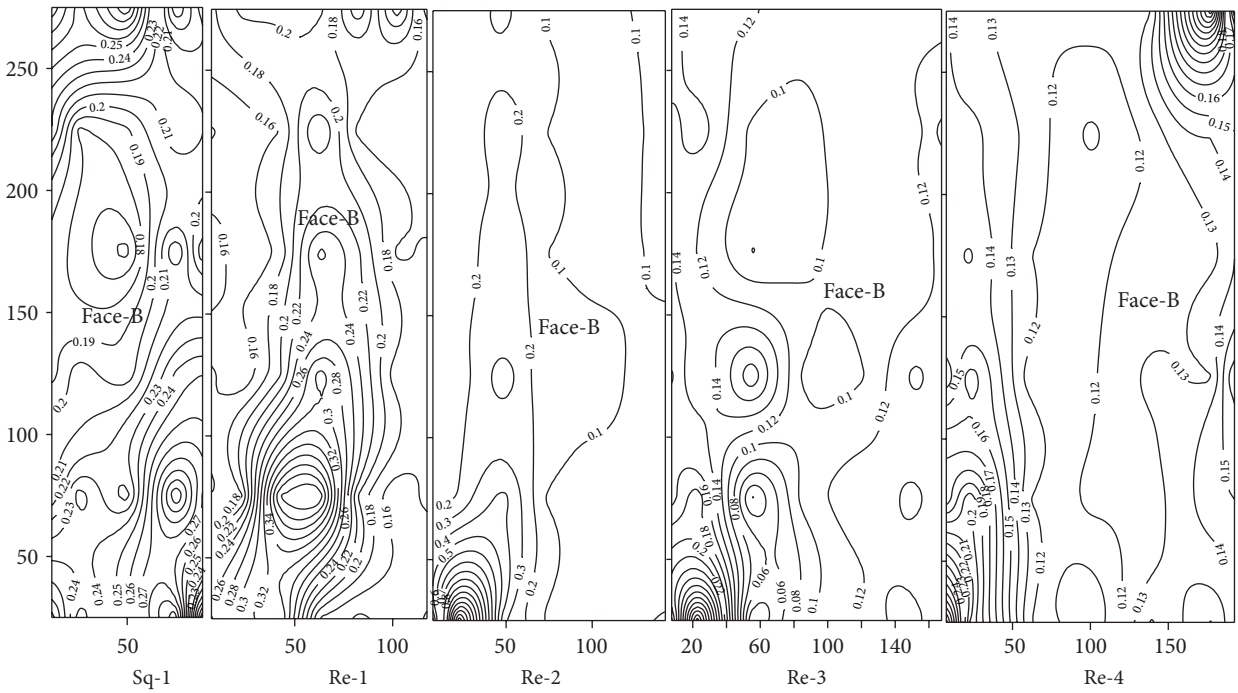

Figure 11: r.m.s. surface pressure coefficient distribution on face-B (angle 15°).

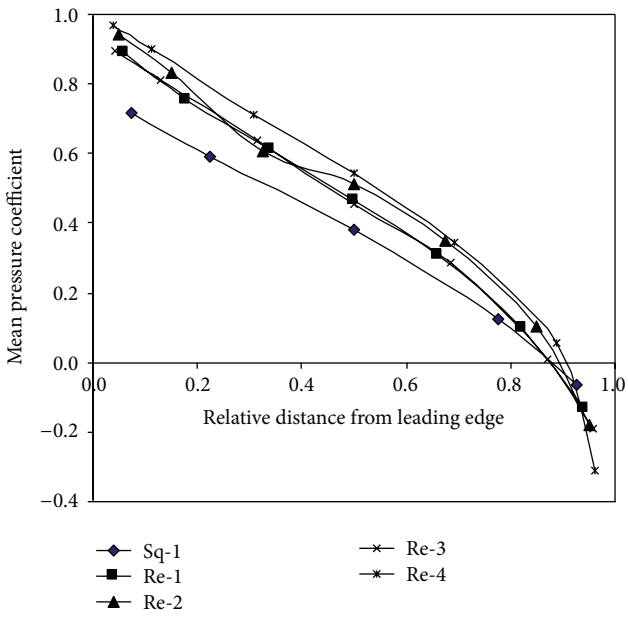

Figure 12: Mean pressure coefficients across section x-x on side face-B at 45° wind incidence angle.

of 0° and 90°. The evaluated force is nondimensionalized to evaluate the force coefficients along the wind direction by $1/2\rho V^2 A_e$, where ρ is the density of air (1.2 kg/m^3), V is the free stream velocity at the roof level of the building model, and A_e is the effective frontal area. The evaluated force coefficients are presented and compared with the results of Lin et al. [14] in Table 4. From the comparisons of force coefficient and pressure contours of rectangular models at wind incidence angle of 0° and 90°, it is observed that magnitude and distribution of the mean wind pressure coefficients on windward faces is almost independent of the side ratio and model depth. Therefore, increase in force coefficient of building models Re-1 (side ratio = 1.56) to Re-4 (side ratio = 4) at wind incidence angle of 90° is caused mainly due to increases in rear-wall suction at wind incidence angle of 90° as compared to wind incidence angle of 0°.

4. Conclusions

The experimental measurement of wind pressures on building models leads to identification of the influence of side ratios and wind orientations on wind pressure distribution and magnitude of pressure coefficients on rectangular building models. At 0° wind incidence angle, the magnitude and distribution of pressure coefficients on windward wall of the rectangular models are almost independent of model depth and side ratio. The absolute value of mean and r.m.s. pressure coefficients on leeward face increases up to side ratio of 0.64. Beyond this critical side ratio, the absolute values of mean and r.m.s. pressure coefficient on leeward face decrease with increase of side ratio. The negative pressure coefficient on leeward face becomes almost constant as the side ratio that exceeds 3.0, indicating that when depth is about three times the breadth, the lower limit of the wake width, which is approximately the full width of the body, is obtained. As the side ratio of models approaches to about 3.0, the final steady reattachment of the flow takes place. The regression equation is also proposed to predict the mean pressure coefficients

Table 4: Force coefficients on building models at 0° and 90° wind incidence angle.

	Wind angle	Model Sq-1	Model Re-1	Model Re-2	Mode Re-3	Model Re-4
Experimental	0°	1.30	1.22	1.11	1.04	0.98
Lin et al. (2005) [14]	0°	1.30	1.20	1.1	1.07	—
Experimental	90°	1.30	1.35	1.38	1.39	1.40
Lin et al. (2005) [14]	90°	1.3	1.45	1.42	1.42	—

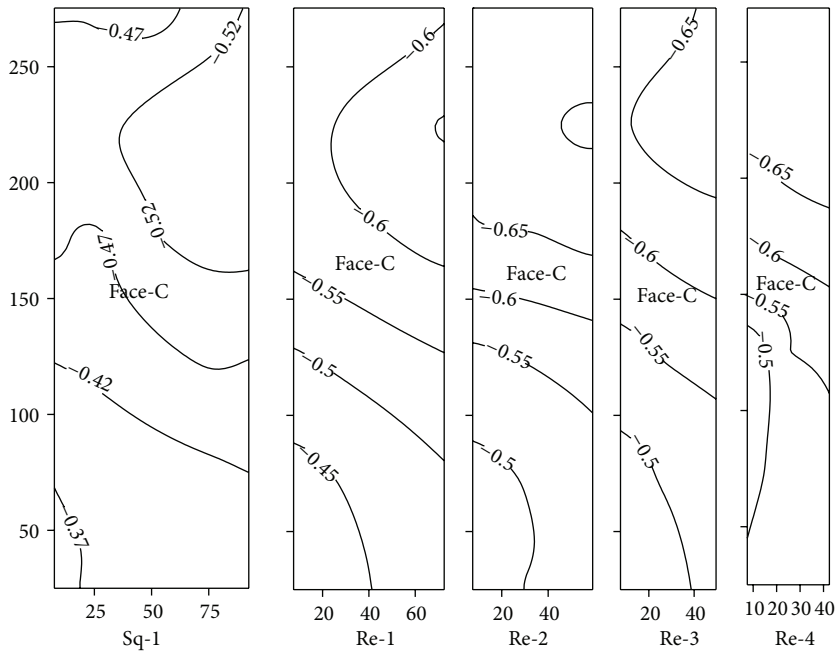

Figure 13: Mean surface pressure coefficient distribution on face-C (angle 45°).

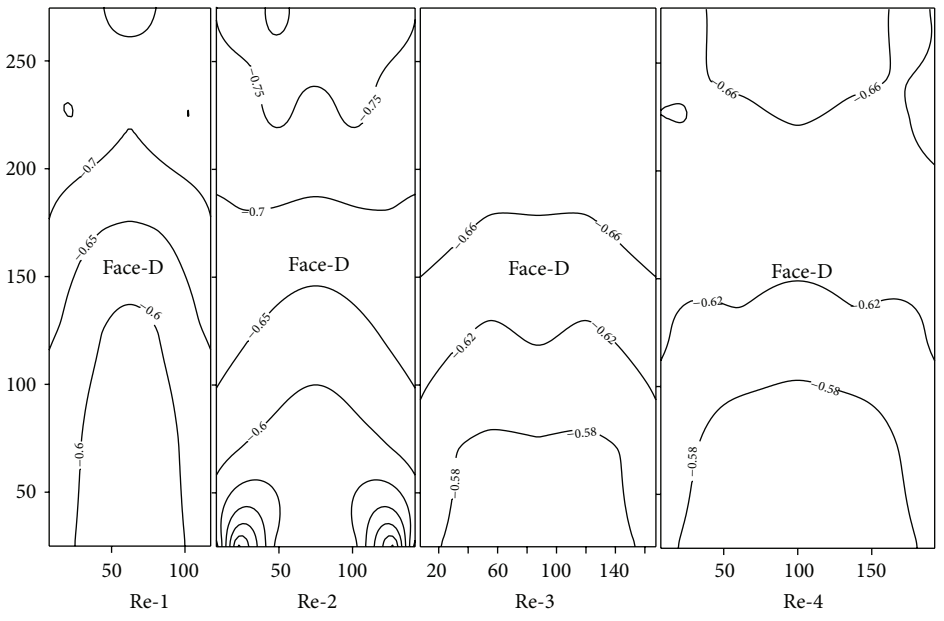

Figure 14: Mean surface pressure coefficient distribution on face-D (angle 90°).

on sidewalls and leeward wall of rectangular models having different side ratios for open country terrain conditions at 0° wind incidence angle. As side ratio of model increases, the absolute value of mean pressure coefficients on side faces decreases from leading edge region to trailing edge region at 0° wind incidence angle. The highest peak suctions may occur practically at any location of the model side face. However, no unusual peak values in excess of –1.59 are found. These may only be associated with more complex model geometrics with more complex surroundings. For building models with constant cross section, change in side ratio does not significantly affect the general magnitude of peak pressures and peak suctions, but rather the wind angle at which they occur.

References

[1] IS: 875 (Part-3), *Code of Practice for the Design Loads (other than earthquake) for Buildings and Structures—Wind Loads*, B.I.S, New Delhi, India, 1987.

[2] AS/NZS:1170.2, *Structural Design Actions, Part-2: Wind Actions*, Standards Australia, Sydney, Australia, Standards New Zealand, Wellington, New Zealand, 2002.

[3] ASCE:7-02, *Minimum Design Loads for Buildings and other Structures*, Structural Engineering Institute of the American Society of Civil Engineers, Reston, Va, USA, 2002.

[4] B. J. Vickery, "Fluctuating lift and drag on a long cylinder of a square cross-section in a smooth and in a turbulent stream," *Journal of Fluid Mechanics*, vol. 25, pp. 481–494, 1966.

[5] B. E. Lee, "The effect of turbulence on the surface pressure field of a square prism," *Journal of Fluid Mechanics*, vol. 69, no. 2, pp. 263–282, 1975.

[6] T. Miyata and M. Miyazaki, "Turbulence effects on the aerodynamic response of rectangular bluff cylinders," in *Proceedings of the 5th International Conference on Wind Engineering*, vol. 1, pp. 631–642, Fort Collins, Colo, USA, 1980.

[7] A. Kareem and J. E. Cermak, "Pressure fluctuations on a square building model in boundary-layer flows," *Journal of Wind Engineering and Industrial Aerodynamics*, vol. 16, no. 1, pp. 17–41, 1984.

[8] P. J. Saathoff and W. H. Melbourne, "The generation of peak pressures in separated/reattaching flows," *Journal of Wind Engineering and Industrial Aerodynamics*, vol. 32, no. 1-2, pp. 121–134, 1989.

[9] A. Kareem, "Measurements of pressure and force fields on building models in simulated atmospheric flows," *Journal of Wind Engineering and Industrial Aerodynamics*, vol. 36, no. 1–3, pp. 589–599, 1990.

[10] D. Surry and D. Djakovich, "Fluctuating pressures on models of tall buildings," *Journal of Wind Engineering and Industrial Aerodynamics*, vol. 58, no. 1-2, pp. 81–112, 1995.

[11] Q. S. Li and W. H. Melbourne, "An experimental investigation of the effects of free-stream turbulence on streamwise surface pressures in separated and reattaching flows," *Journal of Wind Engineering and Industrial Aerodynamics*, vol. 54-55, pp. 313–323, 1995.

[12] Q. S. Li and W. H. Melbourne, "The effect of large-scale turbulence on pressure fluctuations in separated and reattaching flows," *Journal of Wind Engineering and Industrial Aerodynamics*, vol. 83, pp. 159–169, 1999.

[13] Y. M. Kim, J. E. Cho, and H. Y. Kim, "Acrosswind pressure distribution on a rectangular building," in *Proceedings of the 2nd Internal Symposium on Wind and Structure*, pp. 333–342, Busan, Republic of Korea, 2002.

[14] N. Lin, C. Letchford, Y. Tamura, B. Liang, and O. Nakamura, "Characteristics of wind forces acting on tall buildings," *Journal of Wind Engineering and Industrial Aerodynamics*, vol. 93, no. 3, pp. 217–242, 2005.

[15] J. A. Amin, *Effects of plan shape on wind induced response of tall buildings [Ph.D. thesis]*, IITR, Roorkee, India, 2008.

[16] A. J. Macdonald, *Wind Loading on Building*, Applied Science Publisher, London, UK, 1999.

[17] Y. Nakamura and K. Hirata, "Critical geometry of oscillating bluff bodies," *Journal of Fluid Mechanics*, vol. 208, pp. 375–393, 1989.